Spectral Perturbation of Small-World Networks with Application to Brain Disease Detection

Chenhui Hu

May 14, 2012

1 Introduction

Many real life systems can be described by complex networks, which usually consist of a large number of nodes and edges. Among these networks, small-world networks[1] are of particular interest since it captures both the order and randomness of the real phenomena, such as that in the social networks, power grids, neural networks, and so on.

In this project, I am trying to apply this model to classify networks generated from human brain. Since small-world networks are essentially random graphs whose adjacency matrices are random matrices, I first study the spectrum of them. Next, I assume that a sampled brain network is perturbed version of an averaged network: either that over people with Alzheimer's disease, or over healthy people. In order to diagnose a new patient, I calculate the spectral correlation (*i.e.*, correlation of eigenvalue distributions) between the network of this patient and sampled networks in a database, where we know each data point is generated from whether a sick or healthy person. These correlations are then used to determine the status of the patient, which is effective when ówe only have a relative small database compared against the dimension of each network. Apart from this, I also briefly mention an extension of the small-world network model to fit the observed brain networks.

2 Spectra of Small-World Networks

In general, a small-world network refers to a type of mathematical graph where most nodes are not neighbors of one another, while most of them can be reached

Figure 1: Diagram showing the relation among small-world network, regular network, and random network[1].

from every other by a small number of hops [10]. Recently, a variety of phenomena are revealed to be featured with small-world behavior, in mathematics, physics and sociology. Thus, it is important to study the spectra of this type of networks.

2.1 Network Construction

The small-world network is constructed by randomly rewiring a certain amount of the edges of a regular ring network. First, we create a regular ring network as follows. We draw the nodes indexed by $1, 2, \cdots, N$ along a circle in ascending order and for each node i, connect it to the k closest nodes to it: namely nodes $i - k/2, \cdots, i - 1, i + 1, \cdots, i + k/2$, where k is an even number and the arithmetic should be carried out modulo N. Next, starting from node 1 and proceeding towards node N, perform the *rewiring step*. For node 1, consider the first "forward connection," *i.e.*, the connection to node 2 since it is the first connection with end-point index greater than 1. With probability p, reconnect node 1 to another node chosen uniformly at random and without allowing self-loop and multiple edges. Proceed toward the remaining forward connections of node 1, and then perform this step for the remaining $N - 1$ nodes as well. The rewiring for every edge is independent. Fig. 1 shows the relation among small-world network, regular network, and random network. There are $kN/2$ edges in a regular ring network; while in a random network (*a.k.a.*, Erdős-Rényi graph), since every pair of nodes has a probability p to be connected, the expected total number of edges is pN. In a small-world network, there will be $pkN/2$ edges get rewired on average with a rewiring probability p. When p varies from 0 to 1, the small-world network switches from a regular network to a random network, as we see from Fig. 1.

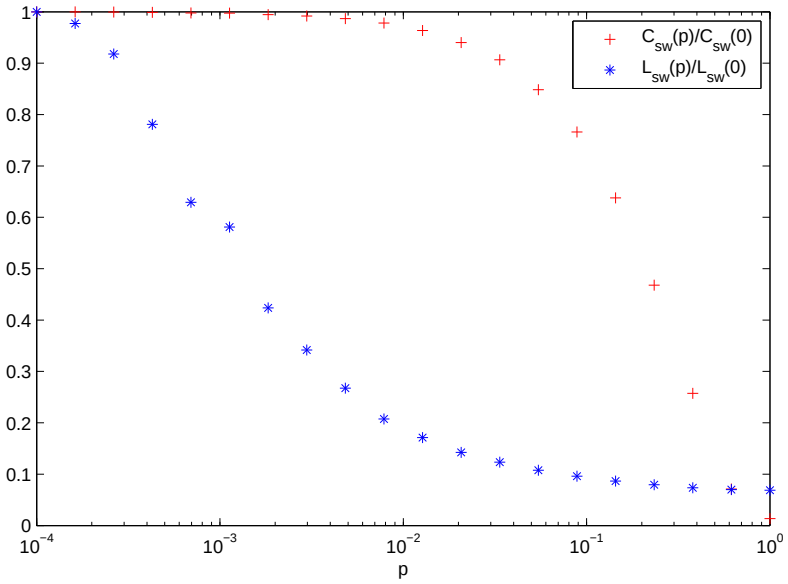

Figure 2: The characteristic path length $L_{\rm sw}$ and clustering coefficient $C_{\rm sw}$ against p ranging from 10^{-4} to 1. The data are averages over 20 random realizations of rewiring and are normalized by dividing their values at $p = 0$, respectively.

As pointed out by Watts and Strogatz, a small-world network is featured with short characteristic path length and large clustering coefficient. Specifically, the characteristic path length $L_{\rm sw}$ is the average shortest path length between every pair of nodes; the clustering coefficient $C_{\rm sw}$ is the fraction of pairs of neighbors of a node which are also neighbors to each other. In a small-world network, the rewired edges act as shortcuts, making the average distance between every two nodes much small. Meanwhile, since it is based upon a regular network, it also has a large clustering coefficient. To illustrate these properties, I recover the classic figure in the seminal paper [1] by plotting $L_{\rm sw}$ and $C_{\rm sw}$ with respect to different rewiring probability p. The number of nodes N and the degree of each node k is fixed as 1000 and 10 respectively, while p is varying from 10^{-4} to 1. Each data point in Fig. 2 is produced by averaging over 20 random realizations of rewiring. We observe that in a certain range of p, roughly from 10^{-3} to 10^{-1}, the characteristic path length is small and the clustering coefficient is large, meaning that the network has a small-world behavior.

2.2 Spectral Properties

The eigenvalue spectrum of complex networks provides insightful information about their structure properties [2]. Thus, in this section, I plot the eigenvalue distribution of small-world network under certain cases. In particular, I choose to study the eigenvalues of the normalized Laplacian matrix $\mathcal{L}$ of the network. Suppose the adjacency matrix $A = (a_{ij})$ is defined as $a_{ij} = 1/0$ if node i and node j are connected or not. And the degree matrix D is a diagonal matrix with elements in the diagonal be the degree of each node. Then, we have

$$\mathcal{L} = I - D^{-1/2} A D^{-1/2}, \tag{1}$$

where I is identity matrix. Again, here I fix $N = 1000$, $k = 10$ and choose $p = 0, 0.01, 0.3, 1$ respectively. The results are shown in Fig. 3, where the horizontal axis is eigenvalue λ and the vertical axis is the probability density of it.

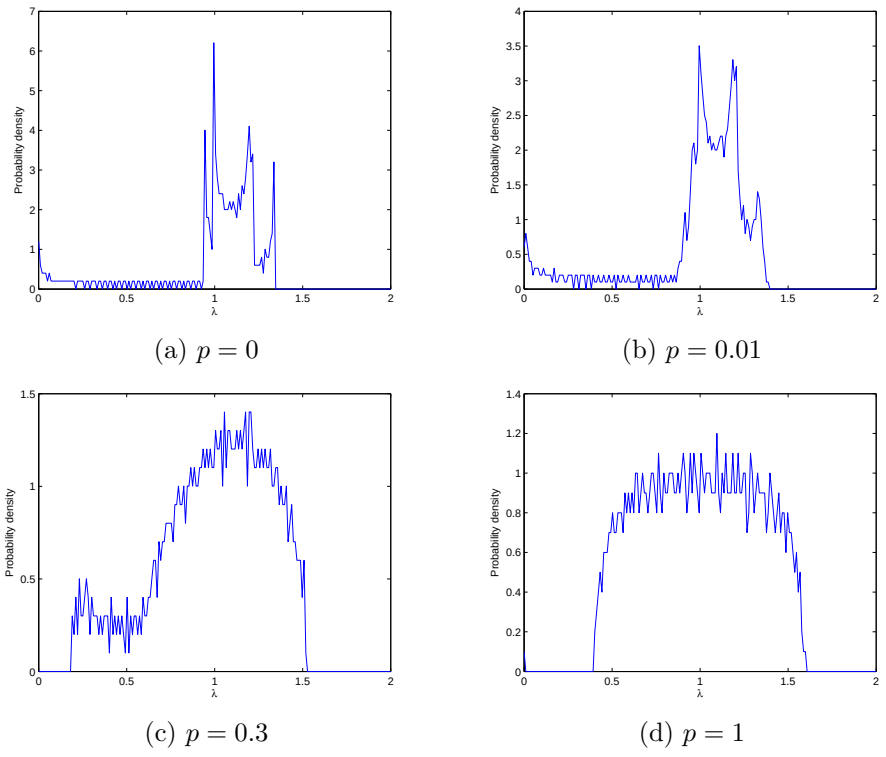

(a) $p = 0$ (b) $p = 0.01$

(c) $p = 0.3$ (d) $p = 1$

Figure 3: Eigenvalue distribution of small-world network with different level of rewiring probabilities p. The number of nodes $N = 1000$ and the degree of each node $k = 10$ are fixed for all four cases.

Fig. 3(a) corresponds to the spectral density of a regular ring network; while Fig. 3(d) corresponds to that of a random network, having a semicircle shape.

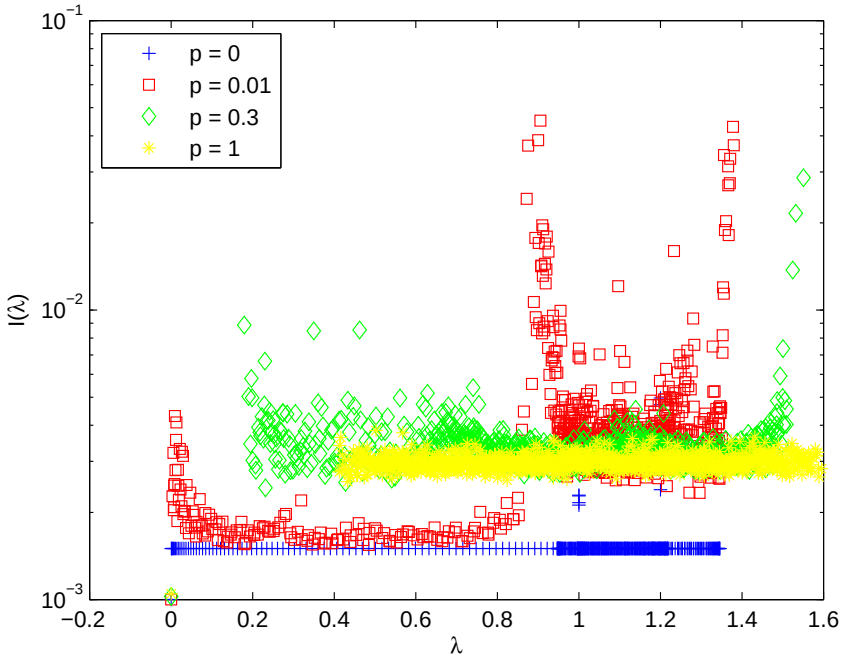

Figure 4: The inverse participation ratios of eigenvectors for small-world networks with different rewiring probability p. $N = 1000, k = 10$ are fixed for all cases.

In Fig. 3(b), we see for $p = 0.01$, the spectral density of the small-world contains sharp peaks, which are the "blurred" remnants of the singularities of the $p = 0$ case. This implies that the network is still near regular, nevertheless containing a small portion of impurities. Fig. 3 shows that for $p = 0.3$, there is not any blurred singularity and the spectrum begins to get close to that of a random network.

Another spectral property that we can look into is the structure of eigenvectors. For instance, in [3] the inverse participation ratio of the normalized eigenvector $v_i = \left(v_i^{(1)}, v_i^{(2)}, \cdots, v_i^{(N)}\right)$ associated with the i-th eigenvalue[1] is defined as

$$I_i = \sum_{j=1}^{N} \left[v_i^{(j)}\right]^4. \tag{2}$$

For an eigenvector whose components are identical, *i.e.* $v_i^{(j)} = 1/\sqrt{N}$ for every

[1] We arrange the eigenvalues in an ascending order.

j, then $I_i = 1/N$. For an eigenvector with one single nonzero component, the inverse participation ratio is 1. From Fig. 4, we observe that the eigenvectors of the regular graph ($p = 0$) and the random graph ($p = 1$) are sparse uncorrelated, although the latter has comparably larger inverse participation ratios. On the contrary, eigenvectors belonging to the small-world network with $p = 0.01$ and $p = 0.3$ are more localized.

3 Perturbation of Small-World Network

As mentioned before, the correlations among a lot of real-life systems can be described by a small-world network. Human brain network is a particular example as discovered in the literature [4] [5] [6]. In this section, I will first illustrate the small-world behavior in this real network. Then, with the assumption that the brain network of a patient is a perturbed version of an averaged network, I determine the status of the patient by comparing the spectral correlation between the observed network and that of people having Alzheimer's disease with the correlation between this network and that of healthy people.

3.1 Brain Network Reconstruction

Alzheimer's disease (AD), as the most common form of dementia, effects over five million Americans and many people around the world. It is a fatal neurodegenerative disorder characterized by progressive impairment of memory and other cognitive functions. Recent advances in neuroimaging techniques, such as Magnatic Resonance Imaging (MRI), Positron Emission Tomography (PET), and Functional MRI (fMRI), offer great potentials for effective discrimination of AD from mild cognitive impairment (MCI), normal aging (NA). It is reported that the disease is closely related to the alternation in the functional brain network, *i.e.*, the functional connectivity among different brain regions [4] [7].

In [7], the authors studied sparse inverse covariance estimation (SICE), *a.k.a.* exploratory Gaussian graphical models, for brain connectivity modeling. Specifically, they applied SICE on PET images averaged over 49 AD, 116 MCI, and 67 NC subjects, respectively. By assuming that the voxel values $\{X_1, X_2, \cdots, X_M\}$ corresponding to different brain regions follow a multivariant Gaussian distribution with mean μ and covariance matrix Σ and letting $\Theta = \Sigma^{-1}$ be the inverse covariance matrix, they formulate the SICE into an optimization problem as follows

$$\hat{\Theta} = \text{argmax}_{\Theta>0} \log(\det(\Theta)) - \text{tr}(S\Theta) - \gamma\|\text{vec}(\Theta)\|_1, \tag{3}$$

where S is the sample covariance matrix; $\det(\cdot), \text{tr}(\cdot)$, and $\text{vec}(\cdot)$ denote the determinate, trace, and sum of the absolute values of all elements of a matrix, respectively. The first two terms $\Big[\log(\det(\Theta)) - \text{tr}(S\Theta)\Big]$ in (3) is the

log-likelihood, while the remaining term $\|\text{vec}(\Theta)\|$ is the sparsity constraint to the inverse covariance matrix. The tradeoff between them is governed by the regularization factor γ.

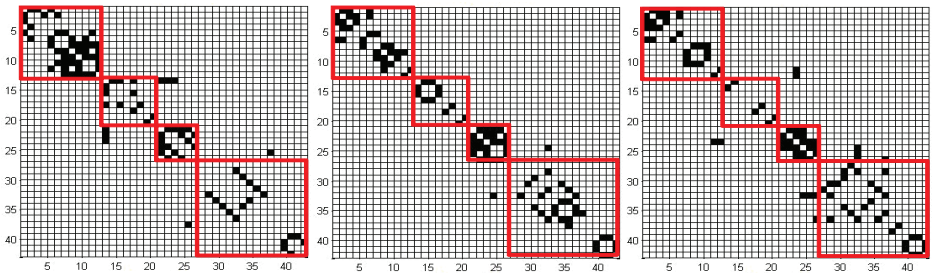

(a) SICE-based brain connectivity networks (total number of edges equal to 50)

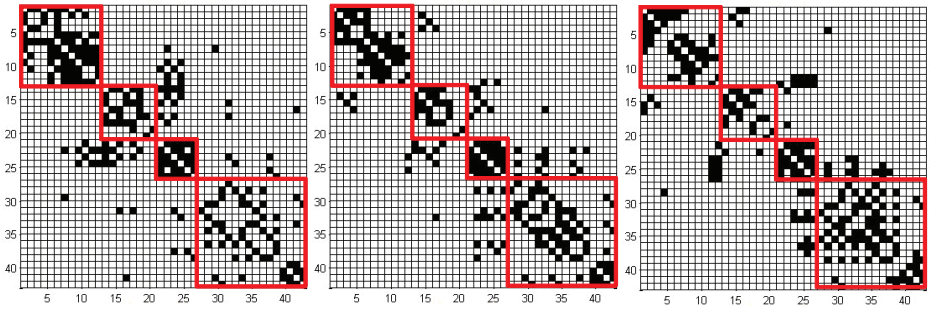

(b) SICE-based brain connectivity networks (total number of edges equal to 120)

Figure 5: Reconstructed brain networks with two different number of edges. The regularization factors for each category of images are adaptively chosen in order to make their amounts of edges identical [7].

Fig. 5 presents the reconstruction results in [7]. Every lattice in the figure illustrates the correlation between two anatomical volumes of interest (AVOI). If the correlation is nonzero, the lattice is marked as dark; otherwise, it is white. The number of edges in each category are made to be even, by adaptively choosing the regularization factor γ. Fig. 5(a) and Fig. 5(b) corresponds to the case when the total number of edges is equal to 50 and 120, respectively. In each subplot, four red cubes are used to highlight the brain regions in each of the four lobes. From top-left to bottom-right, the red cubes highlight the frontal, parietal, occipital, and temporal lobes, respectively. There are indeed difference between AD, MCI, and NC in the connectivity networks. In terms of within-lobe connectivity, for instance, the temporal lobe of AD has significantly less connectivity than NC; while the frontal lobe of AD has significantly more connectivity than NC. In terms of between-lobe connectivity, generally, human

brains tend to have less between-lobe connectivity than within-lobe connectivity, which is a reflection of the small-world behavior. The connectivity between the parietal and occipital lobes of AD is significantly more than NC. Also, AD may have less temporal-occipital connectivity, less frontal-parietal connectivity, but more parietal-temporal connectivity than NC.

3.2 Small-World Feature of Brain Network

The reconstructed brain networks possess the two key features of a small-world network, namely a short characteristic path length and large clustering coefficient. The quantities L_{sw} and C_{sw} associated with networks in Fig. 5 are $L_{\text{sw}} = 1.9365, C_{\text{sw}} = 0.2270$ for AD; and $L_{\text{sw}} = 2.6019, C_{\text{sw}} = 0.3444$ for NC. We may fit the human brain networks with a unified small-world network model. If so, we can classify those networks by their corresponding parameter values in the model. However, notice that the degrees of nodes in brain networks are not always equal and the distribution of the connections of each node is different in terms of the randomness level, we propose the following extended version of the small-world network for fitting human brain networks:

Extension of Small-World Network: First, for each node j in the network we assign a degree k_j to it. The value can be obtained from an estimation according to previous experiment results. In addition, we only require that these k_j nodes are around j, but not necessarily be the closest ones. A shift s_i for the center of the neighborhood range with respect to node j can be adjusted. Next, we add a rewiring probability p_j to the forward edges of node j. This probability is usually different for a different node. In the rewiring step, as that in the classic small-world network, every edge is rewired to an arbitrary node according to the rewiring probability. It turns out that the extended small-world network can also be characterized by a set of parameters (N, k, s, p), with a difference that $k = (k_1, k_2, \cdots, k_N), p = (p_1, p_2, \cdots, p_N)$ are vectors and an additional parameter $s = (s_1, s_2, \cdots, c_N)$.

3.3 Network Classify by Spectral Correlations

We exploit the network classification problem by calculating the spectral correlations in this section. Particularly, I assume that the brain network of a person with Alzheimer's disease is a perturbed version of the averaged network obtained in SICE, and the same holds for a healthy person. We choose the networks of AD and NC with 50 edges in Fig. 5 as the bases. Then, we generate 50 perturbed versions of AD and NC by randomly adding or deleting an edge in the associated bases. Suppose the adjacency matrix of a base network is $A = (a_{ij})$, we determine every entry in the adjacency matrix of a perturbed

network by

$$\widetilde{a}_{ij} = \begin{cases} 1 - a_{ij}, & \text{with prob. } p_t; \\ a_{ij}, & \text{with prob. } 1 - p_t \end{cases} \tag{4}$$

where p_t is the probability of perturbation. After that, we compute the correlation of eigenvalue distributions between the network of a incoming patient and one of that in the database. The patient may belong to the group with Alzheimer's disease or healthy people. Denote the i-th eigenvalue of this new network and that of a network in the database by u_i and v_i, respectively, the spectral correlation is defined as

$$\rho(u, v) \stackrel{\text{def}}{=} \frac{\sum_{i=1}^{N} u_i v_i}{\sum_{i=1}^{N} u_i^2 \sum_{i=1}^{N} v_i^2}. \tag{5}$$

To determine the status of the patient, I compare the average spectral correlations between the new network and the networks of people in two categories and declare that the person belongs to the group with a high average correlation. In this *hypothesis testing* framework, we can study the probability of false alarm P_F and that of missing P_M. Fig. 6 shows the results when $p_t = 10^{-3}$. In this case, P_F and P_M both turns out to be less than 1%. However, I found that if increase the perturbation by a little bit, then those two probabilities will grow quickly. The reason is that the assumed perturbation model is based on every possible edge, the amount of which is very quite large. Thus, a small p_t may make the system unstable.

I also evaluate the hypothesis testing model on the standard small-world networks, as demonstrated in Fig. 7. Notice that $p_t = 0$ corresponds to the base networks without any perturbation. We can see as p_t increases, the blue and red curves get mixed together gradually. Even though, under all three perturbed cases, we have negligible error probabilities P_F and P_M (less than 1%).

4 Conclusion

In this project, I studied the spectral properties of small-world networks and proposed a network classification method by comparing spectral correlations. We model the observation of real networks as perturbed versions of a base network. Experiment results partially confirmed the feasibility of the proposed strategy, although more real data are required to be collected and analyzed in the future.

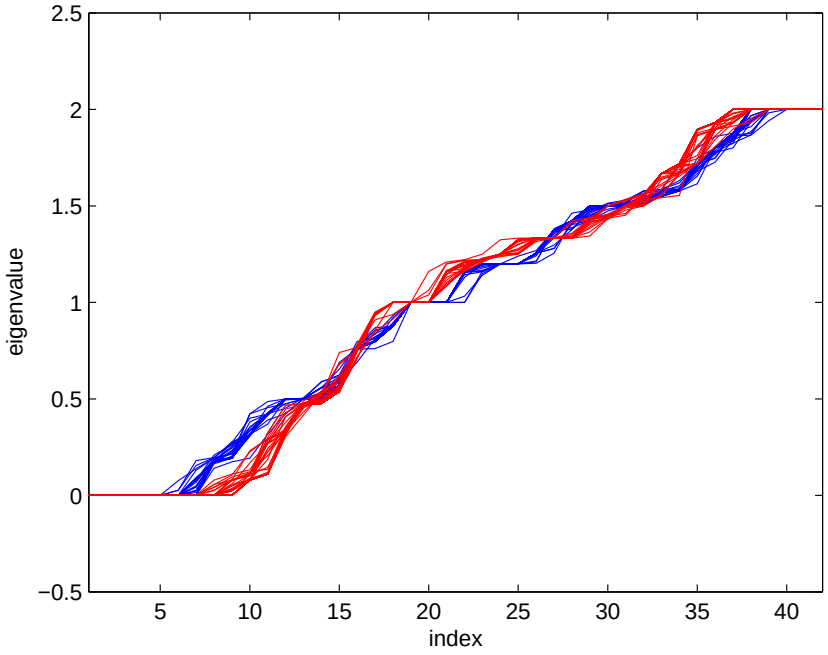

Figure 6: The perturbed eigenvalue distributions for AD (blue lines) and NC (red lines). The perturbation probability p_t for each edge is 10^{-3}.

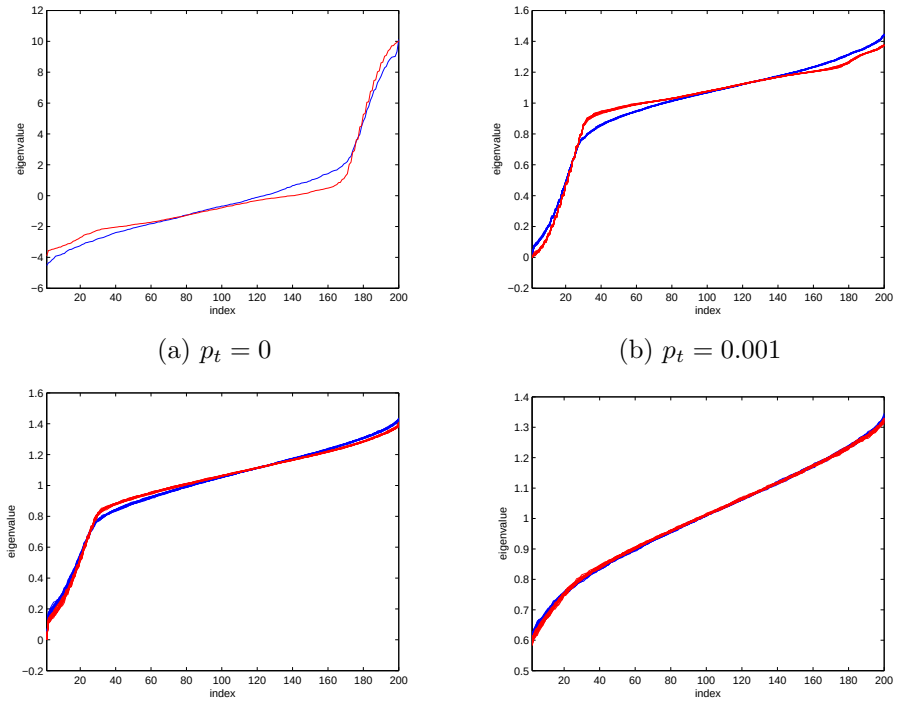

(a) $p_t = 0$ (b) $p_t = 0.001$

(c) $p_t = 0.01$ (d) $p_t = 0.1$

Figure 7: The perturbed eigenvalue distributions of small-world networks with different level of perturbation probabilities p_t. For the base networks, the number of nodes $N = 200$ and the degree of each node $k = 10$ are fixed, while the rewiring probabilities corresponding to blue and red lines are 0.01 and 0.1, respectively.

References

[1] D. J. Watts and S. H. Strogatz, "Collective dynamics of 'small-world' networks," *Nature*, vol. 398, pp. 440-442, 1998.

[2] I. J. Farkas, I. Derenyi, A. L. Barabasi, and T. Vicsek, "Spectra of 'real-world' graphs: beyond the semicircle law," *Phys. Rev. E*, vol. 64, pp. 26704, 2001.

[3] T. Guhr, A. Müller-Groeling, and H. A. Weidenműller, "Random-matrix theories in quantum physics: common concepts," Phys. Rep., vol. 299, pp. 189, 1998.

[4] E. J. Sanz-Arigita, M. M. Schoonheim, J. S. Damoiseaux, S. A. R. B. Rombouts, E. Maris, F. Barkhof, P. Scheltens, C. J. Stam, "Loss of 'small-world'

networks in Alzheimer's disease: graph analysis of fMRI resing-state functional connectivity," *PLoS ONE*, vol. 5, pp. e13788, 2010.

[5] D. S. Bassett and E. Bullmore, "Small-world brain networks," *The Neuro-Scientist*, vol. 12, pp. 512, 2006.

[6] Y. He, Z. J. Chen, and A. C. Evans, "Small-world anatomical networks in the human brain revealed by cortical thickness from MRI," *Cereb. Cortex*, vol. 17, pp. 2407-2419, 2007.

[7] S. Huang, J. Li, L. Sun, J. Liu, T. Wu, K. Chen, A. Fleisher, E. Reiman, and J. Ye, "Learning brain connectivity of Alzheimer's disease by exploratory graphical models," *NeuroImage*, vol. 50, pp. 935-949, 2010.

[8] A. Milanese, J. Sun, and T. Nishikawa, "Approximating spectral impact of structural perturbations in large networks," *Phys. Rev. E*, vol. 81, pp. 046112, 2010.

[9] L. Huang, D. Yan, M. I. Jordan, N. Taft, "Spectral clustering with perturbed data," *Advances in Neural Information Processing Systems (NIPS)*, vol. 21, 2009.

[10] `http://en.wikipedia.org/wiki/Small-world_network`.